

Schramm-Loewner Evolution and isoheight lines of correlated landscapes

N. Posé,^{1,*} K. J. Schrenk,^{2,†} N. A. M. Araújo,^{3,‡} and H. J. Herrmann^{1,4,§}

¹*ETH Zürich, Computational Physics for Engineering Materials,*

Institute for Building Materials, Wolfgang-Pauli-Strasse 27, HIT, CH-8093 Zürich, Switzerland

²*Department of Chemistry, University of Cambridge, Lensfield Road, Cambridge CB2 1EW, UK*

³*Departamento de Física, Faculdade de Ciências, Universidade de Lisboa,*

1749-016 Lisboa, Portugal, and Centro de Física Teórica e Computacional,

Universidade de Lisboa, 1749-016 Lisboa, Portugal

⁴*Departamento de Física, Universidade Federal do Ceará,*

Campus do Pici, 60455-760 Fortaleza, Ceará, Brazil

Real landscapes are usually characterized by long-range height-height correlations, which are quantified by the Hurst exponent H . We analyze the statistical properties of the isoheight lines for correlated landscapes of $H \in [-1, 1]$. We show numerically that, for $H \leq 0$ the statistics of these lines is compatible with *SLE* and that established analytic results are recovered for $H = -1$ and $H = 0$. This result suggests that for negative H , in spite of the long-range nature of correlations, the statistics of isolines is fully encoded in a Brownian motion with a single parameter in the continuum limit. By contrast, for positive H we find that the one-dimensional time series encoding the isoheight lines is not Markovian and therefore not consistent with *SLE*.

PACS numbers: 64.60.al, 89.75.Da, 05.10.-a

We study isoheight lines of long-range correlated landscapes. They are the paths of constant height in topography [1], the equipotential lines on energy landscapes [2, 3], and the constant vorticity lines in turbulent vorticity fields [4]. Empirical and numerical studies of isoheight lines show that they are usually scale invariant [5, 6] and that their fractal dimension d_f depends on the long-range correlations, quantified by the Hurst exponent H [7].

One solid framework to study fractal curves in two-dimensions is the Schramm-Loewner Evolution (*SLE*) theory [8]. Accordingly, an *SLE* curve can be mapped onto a one-dimensional Brownian motion of a single parameter in the continuum limit. Establishing that isoheight lines are *SLE* would allow us to generate an ensemble of such curves by simply solving a stochastic differential equation, without generating the entire landscape, and to extend established results from *SLE* to isoheight lines.

We analyze the zero isoheight lines of random surfaces of different H generated with free boundary conditions on a triangular lattice of size $L_x \times L_y$ with $L_x > L_y$. We consider *chordal* curves that are non-self-touching curves growing to infinity in the upper half-plane \mathbb{H} , starting at the origin. From the Riemann mapping theorem, there is a unique conformal map g_t that iteratively maps the complement of such a curve in the upper half-plane \mathbb{H} back onto \mathbb{H} . This map satisfies the Loewner differential equation,

$$\frac{\partial g_t(z)}{\partial t} = \frac{2}{g_t(z) - \xi_t}, \quad (1)$$

with $g_0(z) = z$ and ξ_t a real continuous function, called the driving function. If a curve is *SLE $_\kappa$* then $\xi_t = \sqrt{\kappa}B_t$, where B_t is a standard one-dimensional Brownian motion

and κ is the diffusion constant. We show that, while for $H \leq 0$ the statistics of ξ_t is consistent with a Brownian motion, for $H > 0$, ξ_t is not Markovian and therefore *SLE* cannot be established.

We generate random landscapes on a triangular lattice, by assigning to each lattice site $\mathbf{x} = (x, y)$ a random height $h(\mathbf{x})$, imposing long-range correlations with the following spectrum,

$$S(\mathbf{q}) \sim |\mathbf{q}|^{-\beta_c}, \quad (2)$$

where $\beta_c = 2(H + 1)$ and H is the Hurst exponent. For that, we use the Fourier Filtering Method [9–11] where,

$$h(\mathbf{x}) = \tilde{\mathcal{F}} \left(\sqrt{S(\mathbf{q})} u(\mathbf{q}) \right), \quad (3)$$

where $\tilde{\mathcal{F}}$ denotes the inverse Fourier transform and the $u(\mathbf{q})$ are independent complex Gaussian random variables of mean zero and unitary variance satisfying $u(-\mathbf{q}) = \overline{u(\mathbf{q})}$. With this scheme, one recovers uncorrelated landscapes for $H = -1$ and the discrete Gaussian Free Field (GFF) for $H = 0$ [12].

To obtain the zero isoheight lines, we extract the set of bonds on the dual lattice separating the sites of negative height from the positive ones. We then focus on their accessible perimeter obtained by moving along the isoheight line and shortcutting distances equal to the lattice unit of the dual lattice, i.e., $\sqrt{3}/3$ lattice units of the triangular lattice [7]. Note that, using the formalism of ranked surfaces, one can show that, for $H \leq 0$, these lines correspond to the accessible perimeter of a correlated percolation cluster at the percolation threshold [7, 13]. The accessible perimeters of the zero isoheight lines on the triangular lattice in the case of $H = -1$ and $H = 0$ are analytically tractable and they have been proven to be *SLE $_{\frac{8}{3}}$* and *SLE $_4$* , respectively [8, 14, 15].

SLE and fractal dimension. As proven by Beffara [16], SLE_κ curves are fractals of a fractal dimension d_f that is related to the diffusion coefficient κ by,

$$d_f = \min\left(2, 1 + \frac{\kappa}{8}\right). \quad (4)$$

The fractal dimension d_f of the accessible perimeter of the isoheight lines for different values of H was numerically estimated and even a conjecture was proposed for its dependence on H [6, 7]. Using Eq. (4), this gives a first estimate for the expected values of κ if the curves are SLE , see Table I. To verify if SLE can be established we will compare the κ values calculated from d_f with estimates obtained with two indirect methods, the winding angle and the left-passage probability, and with the one obtained from the direct SLE mapping.

Winding angle. The winding angle of SLE_κ curves follows a Gaussian distribution and the variance scales with κ as,

$$\langle \theta^2 \rangle - \langle \theta \rangle^2 = \sigma_\theta^2 = b + \frac{\kappa}{4} \ln(L_y), \quad (5)$$

where b is a constant and L_y is the vertical lattice size [8, 17, 18]. To verify this relation for each path, we consider the discrete set of points z_i of the path. The winding angle θ_i at each point z_i can be computed iteratively as $\theta_{i+1} = \theta_i + \alpha_i$, where α_i is the turning angle between two consecutive points z_i and z_{i+1} on the path. Duplantier and Saleur computed the probability distribution of the winding angle for random curves using conformal invariance and Coulomb gas techniques [17]. $\kappa/4$ corresponds to the slope of σ_θ^2 against $\ln(L_y)$, see Fig. 1. The estimates of κ are displayed in Table I.

For values near $H = 0$ and $H = 1$, one has less precision on the results, as the system is strongly influenced by finite-size effects, see e.g. Ref. [7]. The results we obtain from the winding angle measurement are, within error bars, in agreement with the previous estimates from the fractal dimension of the accessible perimeter of zero isoheight lines. Indeed, Eq. (5) gives insights into the conformal invariance of the problem [1]. Our results in Fig. 1 give some numerical indication that the accessible zero isoheight lines display conformal invariance, which is a prerequisite for SLE .

Left-Passage Probability. As we simulate the curves in a bounded rectangular domain, we map conformally the isoheight lines into the upper half-plane, using an inverse Schwarz-Christoffel transformation [19], to obtain the *chordal* curve, which splits the system into two sides. For chordal SLE curves, Schramm has computed the probability $P_\kappa(\phi)$ that a given point $z = Re^{i\phi}$ in the upper half-plane \mathbb{H} is on the right-hand side of the curve [20]. This probability only depends on ϕ and is given by Schramm's formula

$$P_\kappa(\phi) = \frac{1}{2} + \frac{\Gamma(4/\kappa)}{\sqrt{\pi}\Gamma(\frac{8-\kappa}{2\kappa})} \cot(\phi) {}_2F_1\left(\frac{1}{2}, \frac{4}{\kappa}, \frac{3}{2}, -\cot(\phi)^2\right), \quad (6)$$

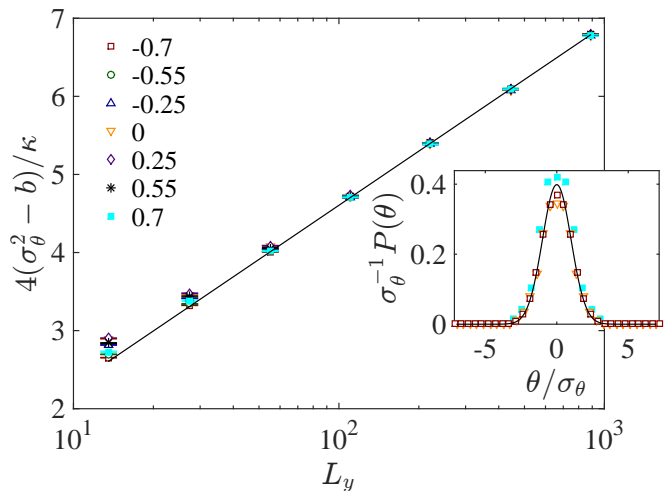


FIG. 1. (color online) Rescaled variance of the winding angle for different Hurst exponents $H = -0.7, -0.55, -0.25, 0, 0.25, 0.55, 0.7$. The black solid line represents the relation $\frac{\sigma_\theta^2 - b}{\kappa/4} = \ln L_y$. In the inset, the rescaled probability distributions are plotted and compared to a normal distribution for $H = -0.7, 0, 0.7$.

where Γ is the Gamma function and ${}_2F_1$ is the Gauss hypergeometric function [21]. This probability is known as left-passage probability.

We define a set of sample points S in \mathbb{H} for which we measure the left-passage probability in order to compare it to the values predicted by Schramm's formula (6). To estimate κ , we minimize the mean square deviation $Q(\kappa)$ between the computed and predicted probabilities,

$$Q(\kappa) = \frac{1}{|S|} \sum_{z \in S} [P(z) - P_\kappa(\phi)]^2, \quad (7)$$

where $\phi = \arg(z)$, $|S|$ is the cardinality of the set S , and $P(z)$ the measured left-passage probability at z . The estimated value of κ corresponds to the point where the minimum of $Q(\kappa)$ is observed.

As shown in Fig. 2, for $H < 0$, the minimum of Q is less pronounced for higher values of H , as it is expected for functions of the form (6) with values of κ increasing towards four. As summarized in Table I, the estimated values of κ obtained for negative H are consistent with the ones predicted from d_f and confirmed by the winding angle analysis. However, for $H > 0$, this is not the case. The obtained κ values do not significantly depend on H and are consistently higher than the ones obtained from d_f . This result suggest that for $H > 0$ the curves are not SLE .

Direct SLE. To further test if the curves are SLE , one has to check that the statistics of the driving function ξ_t is consistent with a one-dimensional Brownian motion with variance κt . This can be done by solving Eq. (1) numerically. In order to do so, we use the so-called vertical

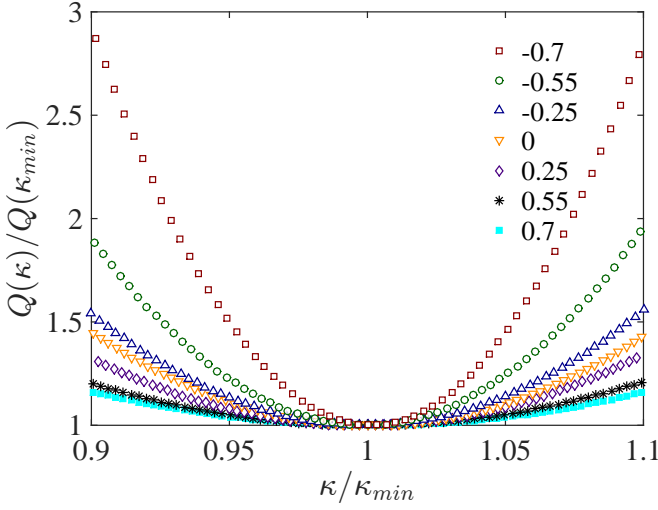


FIG. 2. (color online) Measured rescaled mean square deviation $Q(\kappa)/Q(\kappa_{min})$ as a function of κ/κ_{min} with κ_{min} the value of κ where the minimum of $Q(\kappa)$ is attained, for different Hurst exponents $H = -0.7, -0.55, -0.25, 0, 0.25, 0.55, 0.7$. We chose 50^2 points in the range $[-0.025L_x, 0.025L_x] \times [0.15L_y, 0.25L_y]$ with $L_y = 1024$ and $L_x = 8L_y$, which are then mapped to the upper half-plane through an inverse Schwarz-Christoffel transformation [19].

slit map algorithm, where one considers the driving function to be constant over small time intervals δt . Making this approximation, one can solve Eq. (1) to obtain the following slit map equation [22, 23],

$$g_t(z) = \xi_t + \sqrt{(z - \xi_t)^2 + 4\delta t}. \quad (8)$$

At $t = 0$, one considers the initial curve consisting of the points $\{z_0^0 = 0, \dots, z_N^0 = z_N\}$, and sets the driving function to be $\xi_0 = 0$. Then at each iteration $i = 1, \dots, N$, we apply the conformal map g_{t_i} to the remaining points z_j^{i-1} of the curve, for $j = i, \dots, N$ to obtain the new mapped curve. One gets a new set of points $z_{j+1}^i = g_{t_i}(z_j^{i-1})$ for $j = i, \dots, N-1$ shorter by one point, by mapping z_i^{i-1} to the real axis. For that, in Eq. (8) we set $\xi_{t_i} = \text{Re}\{z_i^{i-1}\}$ and $\delta t_i = t_i - t_{i-1} = (\text{Im}\{z_i^{i-1}\})^2/4$, where $\text{Re}\{\}$ and $\text{Im}\{\}$ are the real and imaginary parts, respectively.

We extracted the driving function of all paths and computed the diffusion coefficient κ , see values in Table I, from the variance of the driving function and tested its Gaussian distribution at a fixed Loewner time t , see Fig. 3. We find a linear scaling of the variance of the driving function with the Loewner time. However, only for $H \leq 0$, the estimated values of κ are consistent with the ones predicted from d_f . For $H > 0$, we obtain values of κ significantly higher than the ones expected from d_f . In fact, the value of κ even increases with H , instead of decreasing as expected.

We also test the Markovian property of the driving function by computing the auto-correlation $c(\tau) =$

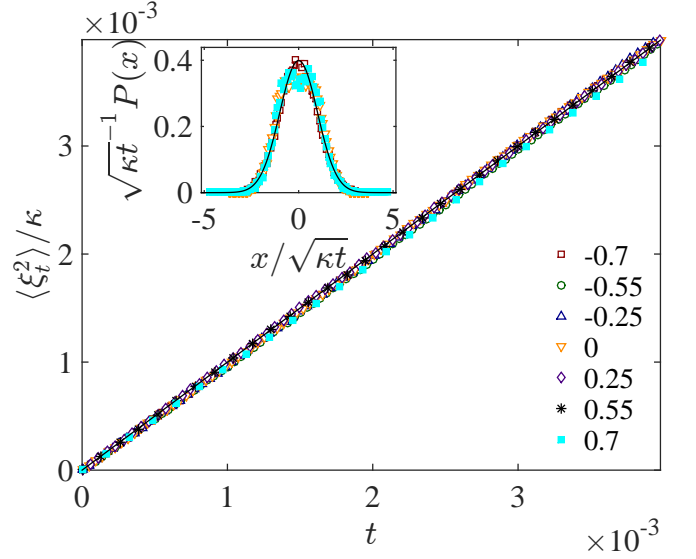


FIG. 3. (color online) Rescaled variance of the driving functions for different values of $H = -0.7, -0.55, -0.25, 0, 0.25, 0.55, 0.7$. In the inset, we present the rescaled probability distributions of the driving functions and compare them to a Gaussian distribution for $H = -0.7, 0, 0.7$.

$\langle c(t, \tau) \rangle_t$ of the increments, with

$$c(t, \tau) = \frac{\langle \delta \xi_{t+\tau} \delta \xi_t \rangle - \langle \delta \xi_{t+\tau} \rangle \langle \delta \xi_t \rangle}{\sqrt{(\langle \delta \xi_{t+\tau}^2 \rangle - \langle \delta \xi_{t+\tau} \rangle^2) (\langle \delta \xi_t^2 \rangle - \langle \delta \xi_t \rangle^2)}}, \quad (9)$$

as shown in Fig. 4, where $\delta \xi_t$ is the change in the driving function at time t . For $H \leq 0$, the correlation function drops to zero after few time steps, as expected for a Brownian motion. For $H > 0$ we observe that the correlation function decays as a power law and thus the driving function is not Markovian, as it shows persistence in the increments. This explains why, though the variance of the driving function is a linear function of time, the statistics of the isoheight lines for $H > 0$ are not consistent with *SLE*.

Conclusion. We numerically showed that the statistics of the accessible perimeter of the zero isoheight lines of long-range correlated landscapes are consistent with *SLE* only for $-1 \leq H \leq 0$. For this range, results for the fractal dimension, winding angle and direct *SLE* are in agreement within error bars, see Fig. 5. This means that one can describe these curves with a Brownian motion parameterized by a diffusivity κ . In the two analytic limits $H = -1$ and $H = 0$, the accessible perimeters are *SLE*_{8/3} and *SLE*₄ for $H = -1$ and $H = 0$, respectively, results that we recover in our numerical analysis. To our knowledge, this is the first time that for an entire range of values of the Hurst exponent H , a family of curves coupled to random landscapes is shown to be consistent with *SLE*. This gives new insight in the field of fractional

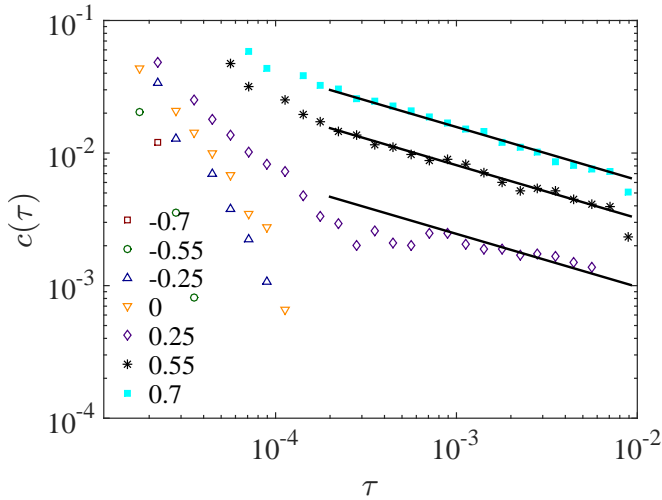


FIG. 4. Auto-correlation function $c(\tau)$ of the increments for different values of $H = -0.7, -0.55, -0.25, 0, 0.25, 0.55, 0.7$, averaged over 50 time steps. The solid lines are power laws of exponent -0.4 .

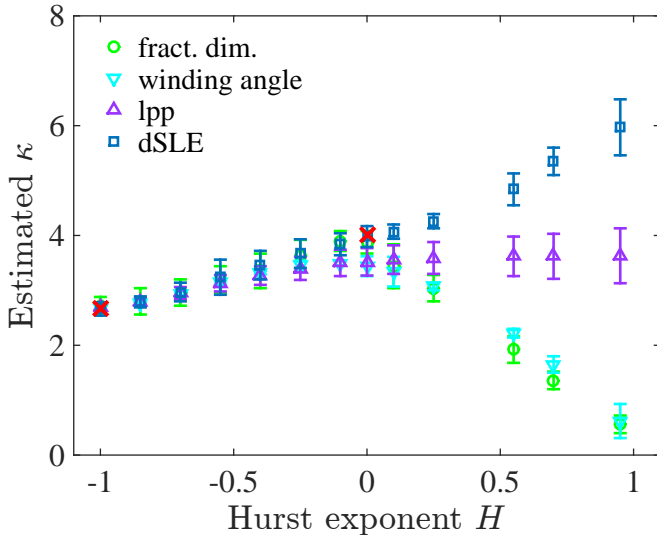


FIG. 5. (color online) Estimated diffusion coefficients κ from the fractal dimension, the winding angle, the left-passage probability (lpp), and the direct *SLE* methods (dSLE). The red crosses correspond to the rigorous results.

Gaussian Fields in two dimensions [12], what might be helpful for understanding correlated landscapes from a theoretical point of view. One might also wonder if these isoheight lines can be related to some random walk process, as in the case of uncorrelated random landscapes and the Gaussian Free Field. For example, the isoheight lines for $H = -1$ and $H = 0$ are two specific cases of the overruled harmonic walker [24].

For positive H , we show that the driving function also scales linearly in time but it is not Markovian, a necessary condition to establish *SLE*. The numerical data suggest

TABLE I. Diffusion coefficient κ computed from the fractal dimension κ_{frac} using data from [7] for $H \leq 0$ and obtained numerically for $H > 0$ using the yardstick method, from the winding angle κ_{θ} , from the left-passage probability κ_{LPP} and the direct *SLE* method κ_{dSLE} , for the different values of the Hurst exponent H .

H	κ_{frac}	κ_{θ}	κ_{LPP}	κ_{dSLE}
-1	2.76 ± 0.16	2.66 ± 0.01	2.69 ± 0.08	2.66 ± 0.12
-0.85	2.80 ± 0.24	2.76 ± 0.02	2.80 ± 0.07	2.79 ± 0.10
-0.7	2.96 ± 0.24	2.94 ± 0.03	2.95 ± 0.11	2.97 ± 0.17
-0.55	3.20 ± 0.24	3.14 ± 0.03	3.13 ± 0.15	3.29 ± 0.32
-0.4	3.35 ± 0.31	3.32 ± 0.03	3.27 ± 0.17	3.46 ± 0.26
-0.25	3.64 ± 0.28	3.45 ± 0.09	3.40 ± 0.21	3.67 ± 0.26
-0.1	3.90 ± 0.18	3.49 ± 0.04	3.50 ± 0.24	3.84 ± 0.20
0	3.88 ± 0.20	3.44 ± 0.18	3.52 ± 0.25	3.98 ± 0.19
0.1	3.44 ± 0.40	3.44 ± 0.27	3.56 ± 0.26	4.07 ± 0.13
0.25	3.04 ± 0.24	3.07 ± 0.07	3.59 ± 0.29	4.26 ± 0.13
0.55	1.92 ± 0.24	2.22 ± 0.08	3.62 ± 0.36	4.84 ± 0.29
0.7	1.36 ± 0.16	1.65 ± 0.16	3.62 ± 0.41	5.35 ± 0.25
0.95	0.56 ± 0.16	0.62 ± 0.31	3.63 ± 0.50	5.97 ± 0.51

that the auto-correlation function scales as a power law. Credidio *et al.* showed that if the driving function is a stochastic process with anomalous diffusion, the generated tracers are anisotropic [25]. In the same spirit, it would be of interest to systematically study the statistics of random curves generated from a driving function with persistence and compare them to isoheight lines.

This Letter also opens the possibility of applying *SLE* to the study of landscapes with negative Hurst exponent H . As we have shown, many systems can be considered from the point of view of a landscape, where isoheights are of relevance. Especially, it has been shown that zero vorticity isolines in two-dimensional turbulence are *SLE* [4]. There have been also attempts to extend this result to isolines in a generalized Navier-Stokes equation [26] to study the conformal invariance of a larger class of turbulence problems. It would be interesting to see if a relation between this problem and our results can be drawn for the accessible perimeters of these contour lines.

The authors would like to thank W. Werner for helpful discussions. We acknowledge financial support from the European Research Council (ERC) Advanced Grant 319968-FlowCCS, support by the Swiss National Science Foundation under Grant No. P2EZP2-152188, and the Portuguese Foundation for Science and Technology (FCT) under contracts no. IF/00255/2013, UID/FIS/00618/2013, and EXCL/FIS-NAN/0083/2012.

* posen@ifb.baug.ethz.ch

† kjs73@cam.ac.uk

‡ nmaraujo@fc.ul.pt

§ hjherrmann@ethz.ch

- [1] G. Boffetta, A. Celani, D. Dezzani, and A. Seminara, *Geophys. Res. Lett.* **35**, L03615 (2008).
- [2] J. M. Ziman, *J. Phys. C* **1**, 1532 (1968).
- [3] A. Weinrib, *Phys. Rev. B* **26**, 1352 (1982).
- [4] D. Bernard, G. Boffetta, A. Celani, and G. Falkovich, *Nat. Phys.* **2**, 124 (2006).
- [5] B. B. Mandelbrot, *The Fractal Geometry of Nature* (Freeman, New York, 1983).
- [6] J. Kondev and C. L. Henley, *Phys. Rev. Lett.* **74**, 4580 (1995).
- [7] K. J. Schrenk, N. Posé, J. J. Kranz, L. V. M. van Kessenich, N. A. M. Araújo, and H. J. Herrmann, *Phys. Rev. E* **88**, 052102 (2013).
- [8] O. Schramm, *Isr. J. Math.* **118**, 221 (2000).
- [9] S. Prakash, S. Havlin, M. Schwartz, and H. E. Stanley, *Phys. Rev. A* **46**, R1724 (1992).
- [10] H. A. Makse, S. Havlin, M. Schwartz, and H. E. Stanley, *Phys. Rev. E* **53**, 5445 (1996).
- [11] B. Ahrens and A. K. Hartmann, *Phys. Rev. B* **84**, 144202 (2011).
- [12] A. Lodhia, S. Sheffield, X. Sun, and S. S. Watson, *arXiv:1407.5598v1*.
- [13] K. J. Schrenk, N. A. M. Araújo, J. S. Andrade Jr., and H. J. Herrmann, *Sci. Rep.* **2**, 348 (2012).
- [14] S. Smirnov, *C. R. Acad. Sci. Paris I* **333**, 239 (2001).
- [15] O. Schramm and S. Sheffield, *Acta. Math.* **202**, 21 (2009).
- [16] V. Beffara, *Ann. Probab.* **36**, 1421 (2008).
- [17] B. Duplantier and H. Saleur, *Phys. Rev. Lett.* **60**, 2343 (1988).
- [18] B. Wieland and D. B. Wilson, *Phys. Rev. E* **68**, 056101 (2003).
- [19] N. Posé, K. J. Schrenk, N. A. M. Araújo, and H. J. Herrmann, *Sci. Rep.* **4**, 5495 (2014).
- [20] O. Schramm, *Electron. Commun. Probab.* **6**, 115 (2001).
- [21] K. J. Schrenk and J. D. Stevenson, *arXiv:1502.05624*.
- [22] T. Kennedy, *J. Stat. Phys.* **137**, 839 (2009).
- [23] J. Cardy, *Ann. Phys. (N.Y.)* **318**, 81 (2005).
- [24] A. Celani, A. Mazzino, and M. Tizzi, *J. Stat. Mech.* , P12011 (2009).
- [25] H. F. Credidio, A. A. Moreira, H. J. Herrmann, and J. S. Andrade Jr., *arXiv:1308.5692*.
- [26] G. Falkovich and S. Musacchio, *arXiv:1012.3868v1*.